ISSN 0190-2717, Bulletin of the Crimean Astrophysical Observatory, 2008, Vol. 104, pp. 67–78. © Allerton Press, Inc., 2007.
Original Russian Text © R.K. Zhigalkin, G.V. Rudenko, N.N. Stepanian, V.G. Fainshtein, N.I. Shtertser, 2008, published in Izvestiya Krymskoi Astrofizicheskoi Observatorii, 2008, Vol. 104, pp. 94–109.

Motions and Magnetic Fields in Filaments

R. K. Zhigalkin[a], G. V. Rudenko[b], N. N. Stepanian[a], V. G. Fainshtein[b], and N. I. Shtertser[a]

[a] *Crimean Astrophysical Observatory, pos. Nauchnyi, Crimea, 98409 Ukraine*
[b] *Institute for Solar–Terrestrial Physics (ISTP), Russian Academy of Sciences, Siberian Branch, P.O. Box 291, Irkutsk, 664033 Russia*

Received February 14, 2008

Abstract—Based on the developed method of jointly using data on the magnetic fields and brightness of filaments and coronal holes (CHs) at various heights in the solar atmosphere as well as on the velocities in the photosphere, we have obtained the following results:
—The upward motion of matter is typical of filament channels in the form of bright stripes that often surround the filaments when observed in the HeI 1083 nm line.
—The filament channels observed simultaneously in Hα and HeI 1083 nm differ in size, emission characteristics, and other parameters. We conclude that by simultaneously investigating the filament channels in two spectral ranges, we can make progress in understanding the physics of their formation and evolution.
—Most of the filaments observed in the HeI 1083 nm line consist of dark knots with different velocity distributions in them. A possible interpretation of these knots is offered.
—The height of the small-scale magnetic field distribution near the individual dark knots of filaments in the solar atmosphere varies between 3000 and 20000 km.
—The zero surface separating the large-scale magnetic field structures in the corona and calculated in the potential approximation changes the inclination to the solar surface with height and is displaced in one or two days.
—The observed formation of a filament in a CH was accompanied by a significant magnetic field variation in the CH region at heights from 0 to 30000 km up to the change of the predominant field sign over the entire CH area. We assume that this occurs at the stage of CH disappearance.

DOI: 10.3103/S0190271708010105

Key words: Sun, filaments, coronal holes, magnetic fields, motions

1. OBSERVATIONS

We begin a series of works on a comprehensive investigation of filaments and coronal holes (CHs) using simultaneous observations in the HeI 1083 nm (hereafter HeI), Hα, and coronal lines as well as data on the magnetic fields and motions. The presented first part of this work is mainly methodological in character. Its goal is to develop a method of jointly using heterogeneous data, to determine the ranges of quantitative variations in the parameters under study, and, where possible, to reveal peculiarities in the relationships between the filament and CH parameters under study.

In this paper, we used the following materials:

—Solar images in the HeI line obtained with the Universal spectrophotometer attached to the TST-2 telescope at CrAO.

—Maps of the radial magnetic field with a strength from 5 to 150 G constructed at ISTP from data of the Kitt Peak Observatory.

—SOHO/MDI data from the Internet.

—Hα observations of the global network taken from the database on the Internet.

—SOHO observations in the 171 Å line.

Let us briefly consider the methods of obtaining these data and their joint reduction.

The solar images in the HeI 1083 nm line were obtained with the TST-2 telescope by scanning the solar images on the spectrograph slit. At the spectrograph exit, the intensity at the HeI line center was recorded using the Universal spectrophotometer with an infrared photomultiplier tube as the detector, an amplifier, and a personal computer. The instrument was described by Stepanian et al. (2000). When the full solar disk and its portions are imaged, the spatial resolution is $10'' \times 10''$ and $2'' \times 2''$, respectively. The spectrograph entrance slit cuts out a 0.12 Å wide spectral region. The full-disk recording time is 15–20 min. Figure 1 shows an example of the solar image in the HeI line obtained by the method described above.

For our analysis, we used the magnetic field calculated above the solar surface using the potential field–source surface model based on the Bd technology (Rudenko, 2001). Its essence lies in the fact that when the Laplace problem for the magnetic field potential is solved, an "instantaneous" (averaged only over the magnetogram measurement time) distribution of the

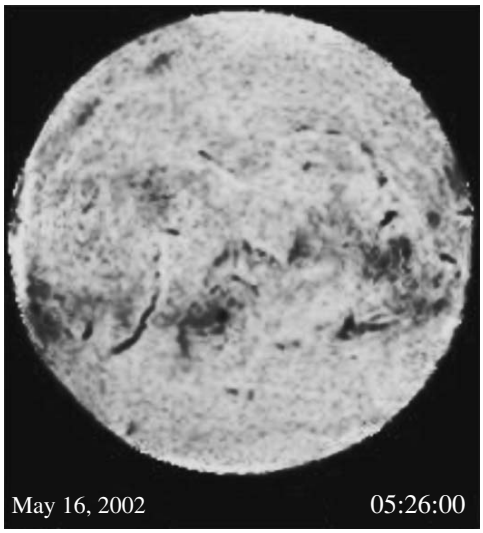

Fig. 1. Solar image in the HeI 1083 nm line obtained with the Universal spectrophotometer attached to the TST-2 telescope at CrAO.

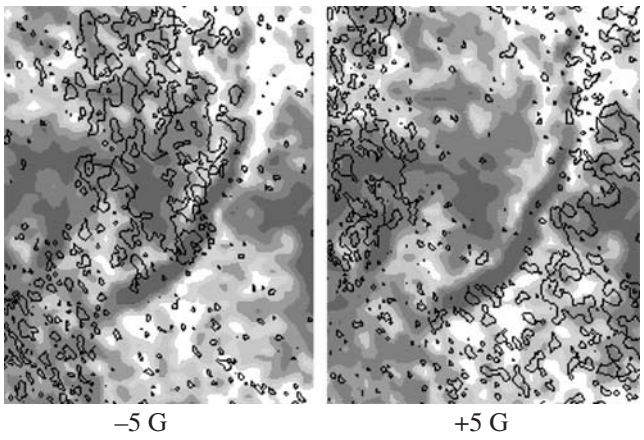

Fig. 2. Portion of the solar image in the HeI line with the plotted Br = –5 and +5 G isolines at the level of magnetic field measurement.

measured longitudinal magnetic field component of the photosphere (Bd component) is used as the boundary condition on the entire visible solar surface. In this case, high-spatial-resolution magnetograms are used. Before September 2003, these were mostly the magnetograms taken at National Solar Observatory/Kitt Peak (NSO). Here, we performed our calculations using also SOHO/MDI magnetograms. This method allows "instantaneous" magnetic field distributions above the visible solar surface to the source surface to be obtained. The radius of the source surface in our calculations is $R_S = 2.5R_0$ (R_0 is the solar radius).

For each day of observations, the distributions of the radial magnetic field with field polarity were plotted on the solar image in the HeI line. The positive (+) and negative (–) polarities correspond to the direction away from and toward the Sun, respectively. We corrected the coordinates for the difference between the times of HeI and magnetic field measurements. We used data with a 5-G interval from 0 to ±100 G. Figure 2 shows a portion of the HeI line image with the plotted isolines of the calculated radial photospheric magnetic field component Br with strengths of –5 and +5 G.

In addition, we calculated the locations of the zero line (polarity reversal line) of the radial magnetic field at heights from 3000 to 30000 km above the level of magnetic field measurement for several days of observations of the CH with the filament formed in it and one extended filament.

The line-of-sight velocities were obtained with the SOHO/MDI instrument. The velocity was corrected for the solar rotation using a technique described by Zhigalkin (2007). Figure 3 shows a map of the line-of-sight velocities on the Sun corrected for the solar rotation. In this map, we see a cellular structure and an increase in contrast when passing from the center of the solar image to its edges.

During the subsequent processing of the velocity distributions over the solar disk, we subtracted the hourly mean velocity over the entire disk from the hourly mean velocity in each portion of the solar disk under study.

The solar images in the Hα and 171 Å lines taken from the Internet were reduced to the image size in the

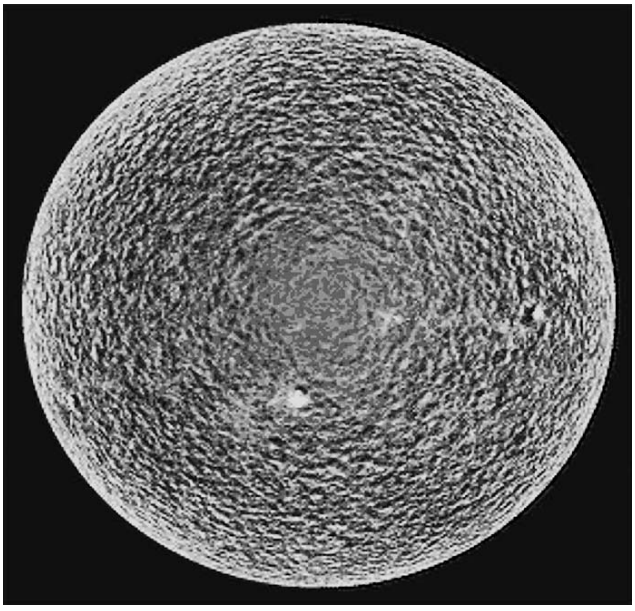

Fig. 3. MDI/SOHO map of line-of-sight velocities on the Sun corrected for the solar rotation.

Filaments observed in the HeI line on May 10–26, 2002

Date / No.	10	11	12	13	14	15	16	17	18	20	22	23	24	26	Notes
1		+	+	+	+	+									Sigmoid
2	+	+	+	+	+	+	+								Extended EW
3	+	+	+	+	+	+	+	+							Emerged in CH
4	+	+	+	+	+	+	+								Y-shaped
5	+	+	+	+	+	+									Curved
6	+	+	+	+	+	+									Curved
7	+	+	+	+	+	+									At AR boundary
8	+	+	+	+	+										Extended NS
9	+	+	+	+	+										Extended NS
10	+	+	+	+	+										Curved
11	+	+	+	+	+										At AR boundary
12	+			+	+	+	+	+	+	+					Extended NS
13				+	+	+	+	+	+	+					At AR boundary
14						+	+	+	+						Short EW
15							+	+	+						Short NS
16							+	+	+	+	+	+	+		Extended NS
17										+	+	+	+		Extended EW
18										+	+				Extended NS
19											+	+	+	+	Extended EW
20												+	+	+	Short EW
21												+	+	+	Extended NS
22													+	+	Short NS

HeI line. The spatial resolution of these images is 1″–2″.

Once the images of all types have been reduced to the same size, time of observations, and coordinate system, the subsequent processing was performed using the multifunction IDL software package described by Stepanian et al. (2000).

The method of a joint data analysis was tested on the May 10–26, 2002 observations. We traced the fate of 22 filaments using the solar images in the HeI line with the superimposed magnetic field and velocity observations. The 171 Å line and Hα observations were invoked. The table gives a list of these filaments for all days of observations with brief notes.

When observed in the HeI line, all filaments can be roughly divided into three classes by their associations with the surrounding solar structures:

(1) the filaments separating the structures of background magnetic fields of opposite signs;

(2) the filaments associated with active regions (connecting active regions, ring ones, sigmoid ones, etc.);

(3) the filaments associated with CHs (located entirely inside CHs, one end of a filament inside or at the boundary of a CH, a filament crossing a CH).

Most of these filaments are also seen in the Hα line, but there are cases where the filament is present in the HeI line and absent in Hα.

2. FILAMENT CHANNELS IN THE HeI LINE

Let us first consider some of the filament peculiarities based on the HeI line observations. The bright stripes elongated along the filaments and observed near most of the filaments are the first thing to catch the eye (an example of these stripes is shown in Fig. 4). These stripes in the HeI line are known to be formed by filament channels (Harvey and Gaizauskas 1998)—the structures in the solar atmosphere within which the filaments are located. These channels are located along the polarity reversal line of the photospheric magnetic field (Harvey and Gaizauskas, 1998). Note that the properties of the channels observed in the HeI line have been studied poorly so far and performing such studies is topical.

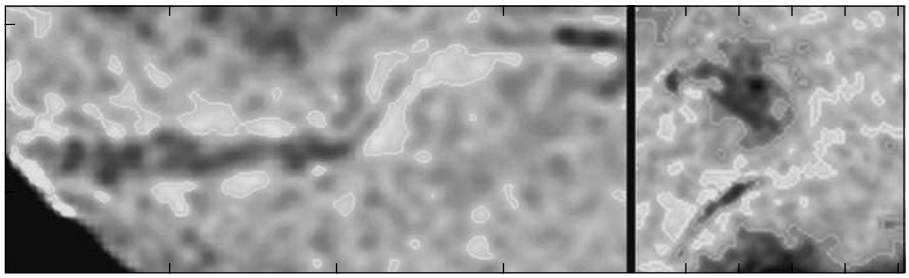

Fig. 4. Images of two solar areas in the HeI 1083 nm line with filaments surrounded by bright stripes—filament channels.

Several types of bright stripes are encountered near filaments. The stripes are seen sometimes on one side, sometimes on both sides. The filament ends outside active regions are often surrounded by a bright region. The shape of the stripes changes as the filaments develop. The bright regions near the filament ends occasionally turn into CHs. The stripe brightness in the HeI line is the same as that in CHs, i.e., the intensity of the emission in them satisfies the relation: $I > 1.01I_{undist}$ (Malanushenko and Stepanian, 1996). The radial field component Br in the stripes at the level of magnetic field measurement is most commonly close to 0. This reflects the above-mentioned fact that the filament channels are located along the polarity reversal line of the photospheric magnetic field. On average, the velocity of matter in the stripes at the level of SOHO/MDI velocity measurement is directed upward. At the same time, the velocity measurements in the filament itself (Filippov, 2007) give a complex pattern of the velocity field. Upward, downward, and horizontal motions are observed in the individual threads comprising the filament. Velocity oscillations and even rotational motions are also observed.

Let us consider three extended (along the meridian) quiet filaments that separate the background fields of opposite signs and their relationship to the bright stripes. These filaments have nos. 9, 12, and 16 in the table. When passing over the disk, they are characterized by a change in the shape of the bright stripes adjacent to them with time.

Filament no. 9 was in the western hemisphere from May 12 to May 14. A bright stripe is adjacent to it on the eastern side.

Filament no. 12 was clearly seen on the disk from May 13 to May 20. On the first days of observations, when the filament was in the east, it had a bright stripe on the western side, at the disk center on both sides, and the stripe was adjacent to the filament from the east in the western hemisphere. A similar picture was observed for filament no. 16 from May 16 to May 24.

These data can be interpreted in the following way. The filament is denser than the filament channel and is optically thick. Because of its appreciable radial extent, the filament overlaps the emission of the eastern part of the channel when it is located to the east of the central meridian and the western part when it is located to the west of the central meridian.

Let us turn to the Hα observations of these filaments. When the filaments are located near the limb, bright stripes are seen near them: from the west and the east when the filament is in the eastern and western hemispheres, respectively. No bright stripes are seen at the disk center. The picture is similar to that observed in the HeI line (Fig. 5).

It follows from the above illustrations that the filament channels in Hα are narrower than those in HeI. It turns out that considerably wider filament channels than those in Hα are also observed in the short-wavelength part of the coronal radiation—in extreme ultraviolet lines (Aulanier and Schmieder, 2002). Note that the brightness of the filament channels in the Hα observations is close to that of flucculi.

Recall once again the well-known and, probably, fundamental property of the filament channels that manifests itself most clearly when observed in the Hα line. Inside the channels, the fibrils are located almost along the zero magnetic field line (or the polarity reversal line) and never cross them (Martin, 1998; Gaizauskas, 1998).

Thus, we found the following:

—According to the HeI line observations, most of the filaments are surrounded by bright stripes—filament channels.

—The channel brightness is comparable to the CH brightness.

—The pattern of change of the channels as the filament is displaced from the east to the west suggests that the filament channels are overlapped along the line of sight by the filament to the east and the west of the central meridian.

—The radial photospheric magnetic field in the filament channels has a strength (in magnitude) ≤5 G. This is consistent with the fact that the filament channels are located along the zero photospheric magnetic

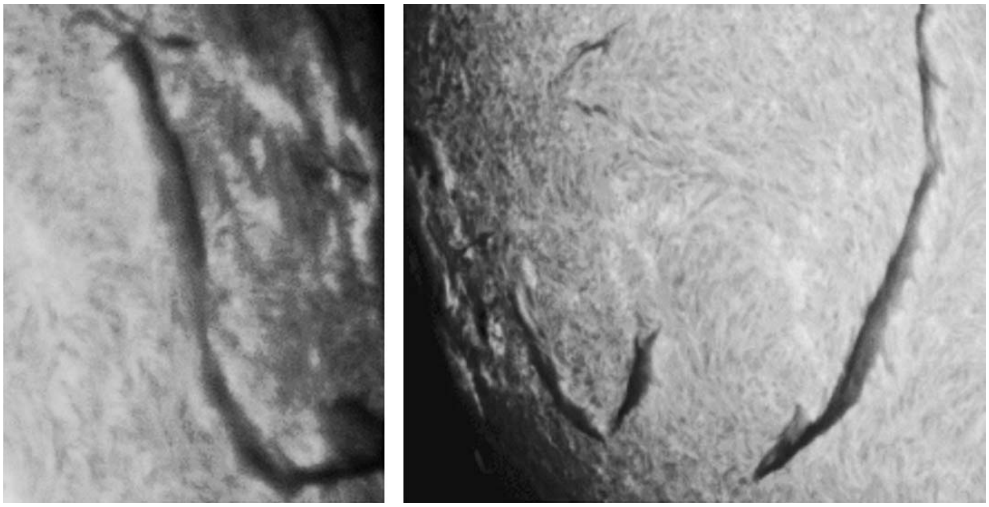

Fig. 5. The same filament near the western (W) and eastern (E) limbs when observed in the Hα line.

field lines. At the same time, it should be kept in mind that the magnetic field in the filament channels when observed in the chromosphere and the lower corona is strongly nonpotential (Martin, 2007). The filament channels turn out to be fairly extended in height and, according to Aulanier and Schmieder (2002), penetrating into the corona.

—In most cases, an upward motion of matter is observed in the filament channels at the level of MDI velocity measurement. Such bright stripes (filament channels) are also seen in Hα near the extended (along the meridian) filaments and have a flocculi brightness of $\approx(1.10–1.15)I_{undist}$.

It also follows from the aforesaid that the filament channels are not such known structures of the solar atmosphere as flocculi. Not only the Hα-to-HeI brightness ratio, but also the nearly zero strength of the radial photospheric magnetic field in the channel region distinguishes them from flocculi. This is consistent with the fact that the fibrils in the filament channels are located almost parallel to the magnetic field polarity reversal line. In contrast, the magnetic field in flocculi measured along the line of sight is stronger than 5 G.

3. EVOLUTION OF THE FILAMENT EMERGED IN A CORONAL HOLE

Let us consider in more detail filament no. 3 from the table that emerged either inside a CH or in the channel adjacent to the northern CH boundary. Its change over several days in the HeI line is presented in heliographic coordinates in Fig. 6. Figure 7 shows the location of this filament on the solar disk on May 15, 2002.

On May 10, 2002, two dark points are seen in or near a small CH. On May 12, 2002, a small filament that appears as being located entirely in the CH emerged at their location.

On the succeeding days, the filament grows through the appearance of new knots and their connection with the old knots. The filament approached the northern CH boundary on May 14, 2002, and connected with the middle part of filament no. 2 lying outside the northern CH boundary on May 15. At the place of the connection, the structure of the filaments changed noticeably and a downward motion of matter was observed.

On the next day, the western part of filament no. 2 was destroyed, while its eastern part connected with filament no. 3 outside the CH and strengthened considerably. On May 17, the filament remained in the form of a chain of dark knots. Approximately the same picture was observed in the Hα images of the Sun. To illustrate the "similarity" of the filament when observed in various chromospheric lines, Fig. 7 shows the HeI (CrAO) and Hα (BBSO) images of the Sun on May 15, 2002.

The filament knots that appeared during the described events were small bipolar magnetic regions whose emergence was accompanied by a change in the directions of motion of matter. In most cases, the directions of motions are opposite at the knot ends.

The CH within which filament no. 3 developed is a peculiar CH. According to Bugaenko et al. (2004), this CH is characterized by a decrease in its area with height.

This follows from a comparison of the CH area in the HeI line with that in various extreme ultraviolet

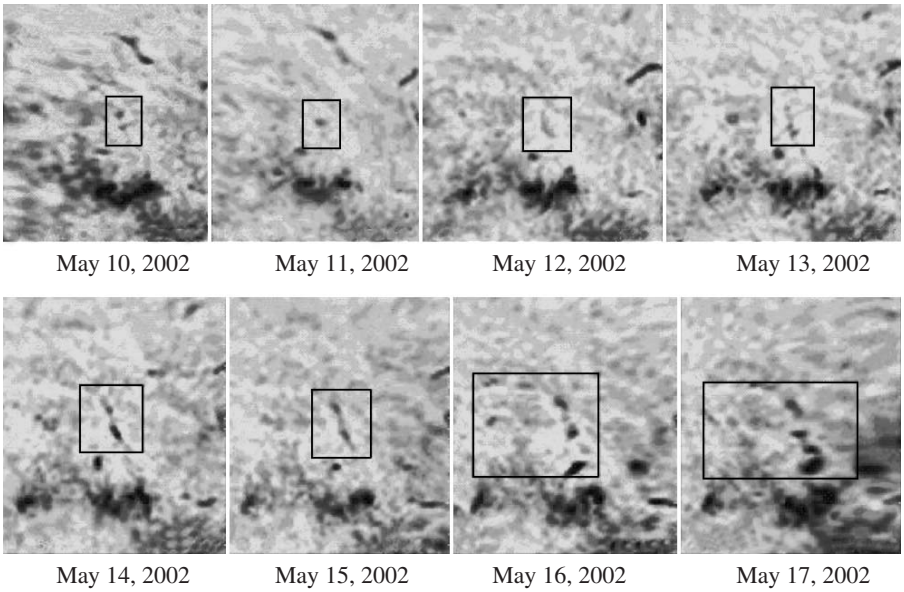

Fig. 6. Change of the filament detected in the HeI line that emerged in or near a CH with time. The image is given in heliographic coordinates.

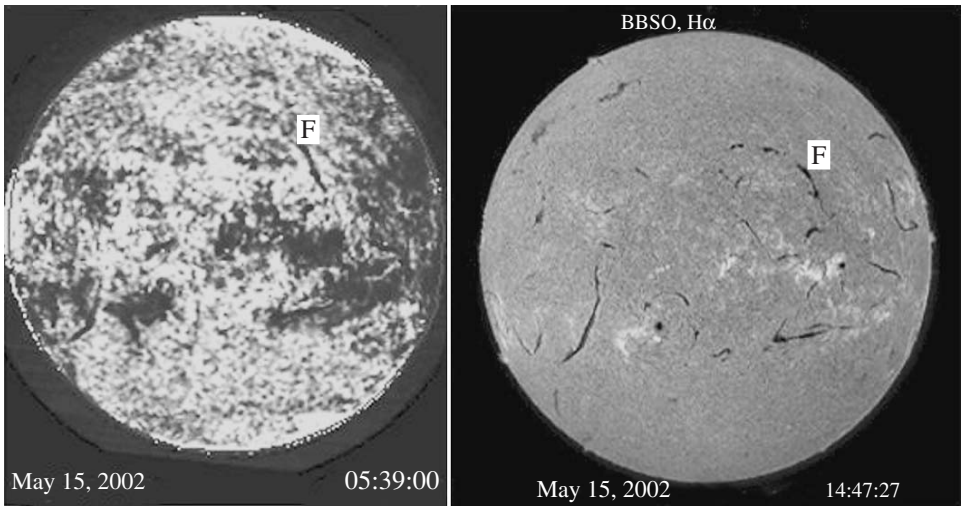

Fig. 7. Filament no. 3 (marked by the letter F) from the HeI 1083 nm and Hα line observations on May 15, 2002.

lines from SOHO/EIT data. This CH is not the location of the footpoints of open magnetic field lines, which is characteristic of "normal" CHs. It is not the source of a fast quasi-steady-state solar wind stream on the Earth's orbit either.

For the May 12–16 observations, in addition to the distribution of the radial photospheric magnetic field (Br) in the CH region, as discussed in the Section "Observations," we calculated the locations of the zero lines (polarity reversal lines) of the small-scale magnetic field at various heights in this CH. The calculations were performed for heights of 3, 5, 10, 15, 20, and 30 thousand kilometers under the assumption of a potential field. In Figs. 8 and 9, the zero lines at these levels are superimposed on the original CH images in the HeI line for May 12 and 16. The two images in the lower row on the right are the isolines of the radial magnetic field Br = –5 and +5 G at "zero" height—at the place of photospheric magnetic field measurement.

Over the period under consideration, the pattern of the magnetic field in the CH changed significantly at all heights.

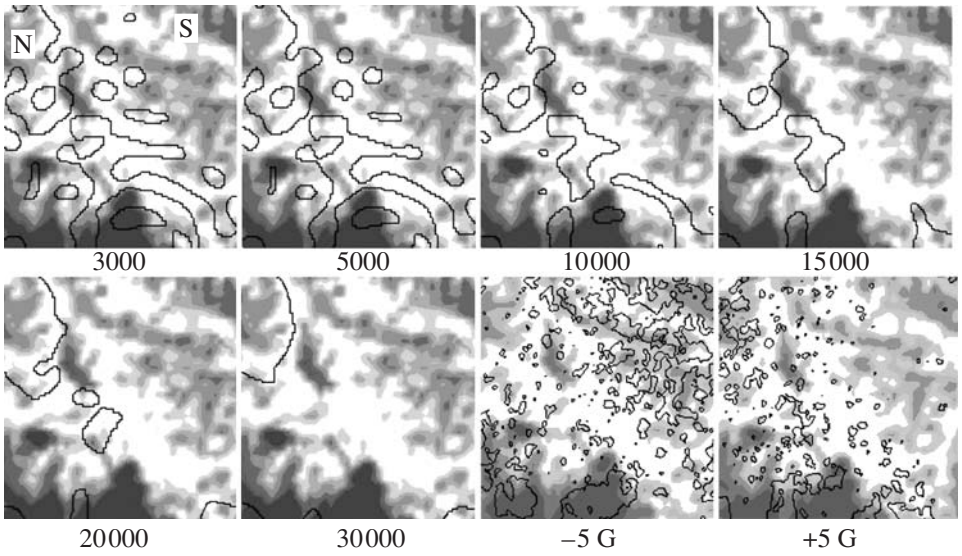

Fig. 8. Zero lines at heights from 3000 to 30000 km superimposed on the solar image in the HeI line for May 12, 2002. The bottom right panels show the isolines of the radial magnetic field with a strength of –5 and +5 G at zero height.

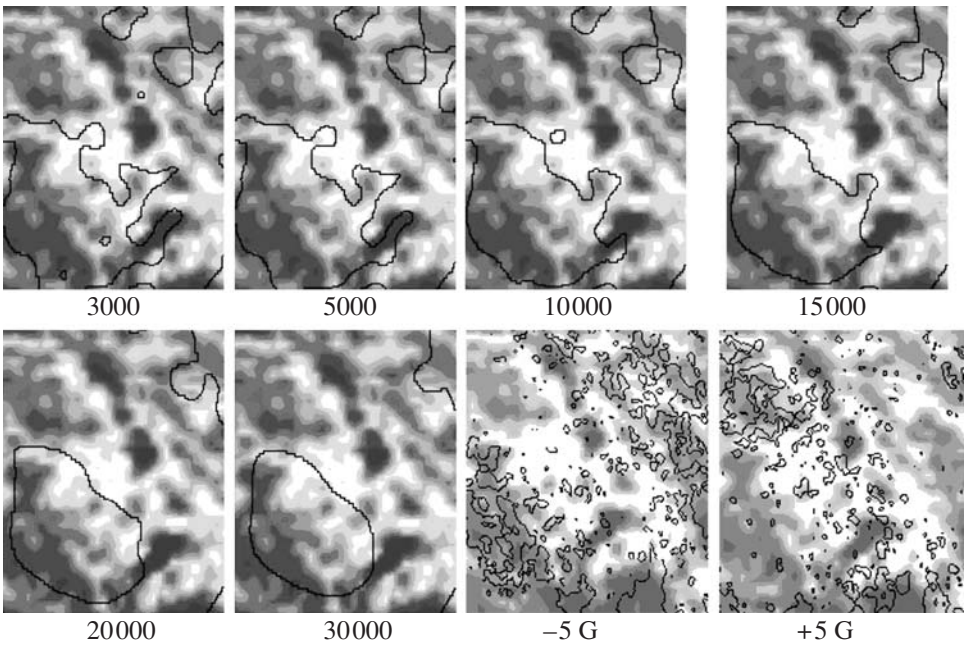

Fig. 9. Same as Fig. 8 for May 16, 2002.

On May 12, the entire CH was covered by N-field inclusions into the background S field. The zero line at heights up to 10000 km crosses the filament several times. This suggests that the filament consists of several bipolar structures most of which extend to 10000 km and, some of them, up to 20000 km. The S field without inclusions of opposite polarity is observed only at 30000 km above the filament. The N-field inclusions above the entire CH behave similarly. The number of inclusions decreases with height and the N field at 30000 km is seen only at the northeastern CH boundary.

For all days of observations and the entire set of heights, we determined the ratios of the areas occupied by the N field to the total area of the distinguished regions (Figs. 10, 11).

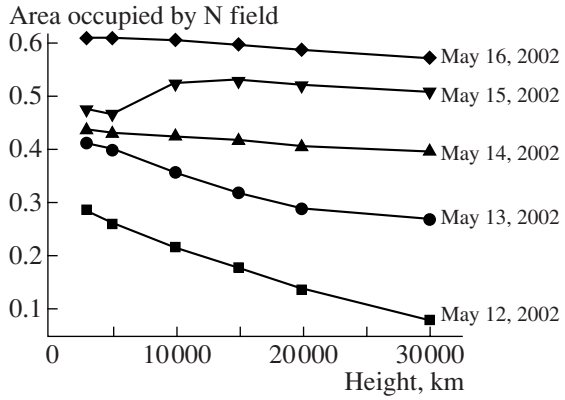

Fig. 10. Variation of the fraction of the distinguished area occupied by the N field with height. Each curve is given for one day of observations.

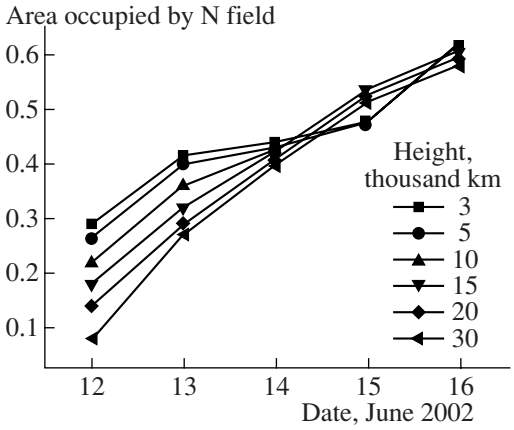

Fig. 11. Variation of the fraction of the distinguished area occupied by the N field with time. Each curve is given for the same height

We see from Fig. 10 that the fraction of the N-field area increases at all heights and before74 May 16 occupies more than half of the area of the distinguished regions and almost the entire CH (see also Fig. 8). The ratio of the N-field areas at different heights (Fig. 11) changes from day to day. Whereas the N-field area at 3000 km on May 12 is almost a factor of 4 larger than that at 30000 km, the N-field fraction on May 16 is almost the same for all heights.

Thus, we found that the ratio of the areas occupied by the N and S magnetic fields changed over 5 days of the CH life at different heights, which essentially led to the change of the predominant field sign at heights from 0 to 30000 km. This probably reflects the observed CH evolution. As has already been noted above, this CH became peculiar starting from May 13, 2002: its area decreased with height and it was not the source of a fast solar wind stream. At the same time, on May 12, 2002, and earlier, this CH was still a "standard" one: its area increased with height. At this time, a certain magnetic field polarity, in the case under consideration, a negative polarity, should predominate in the CH, since a "standard" CH is predominantly the region of open field lines. The predominance of a negative-polarity field in the CH under consideration is confirmed by the set of synoptic maps of the radial magnetic field calculated by the method of Rudenko (2001) and the region of its measurement (Fig. 12). At the same time, we see that near the CH center, the region occupied by negative field polarity decreases between May 10 and May 17. A visual analysis of the brightness around the CH center shows that the area of the region of enhanced brightness in the HeI 10830 Å line images of the Sun slightly decreases with time from May 13 to May 17, 2002. This partly reflects the decrease in the brightness of the CH as it moves toward the limb. However, this is mainly related to the CH destruction, its disappearance, which is indirectly confirmed by the absence of this CH on June 10, 2002, after one solar rotation starting from May 13, 2002. Note that according to the extreme ultraviolet line measurements, the CH area in the lower corona decreased with time and the CH virtually disappeared on May 16, 2002. At the same time, the filament developed in this CH was also observed on June 10, 2002.

Thus, we conclude that, in the case under consideration, the decrease in the fraction of the CH area occupied by the field with predominant polarity reflects the CH destruction, while the development of a filament in the CH is either the result of this destruction or its trigger.

As regards the sharp decrease in the fraction of the CH area occupied by a positive-polarity field with height on May 12 and 13, 2002, it can be explained in the following way. In this period, the CH under consideration had just begun to lose the properties characteristic of a "classical" CH. Hence, it continued to be a region with a predominantly unipolar magnetic field on large spatial scales. Therefore, the fraction of the area with a field of nondominant (positive) polarity is small at the relatively large heights considered (more than 10000 km). However, at the bottom, near the height at which the magnetic field is measured, the small-scale field has both negative and positive polarities and the fraction of the area with positive polarity increases.

When analyzing the line-of-sight velocities in this CH and the filament in it, we found that the distribution of the regions of upward and downward motions changed from day to day.

Thus, the observations showed that the formation of a filament in the CH affected all layers of the solar

atmosphere. In the photosphere, the magnetic fields and the velocity distribution changed. New magnetic fluxes emerged in the chromosphere, the brightness of the CH and the vertical stratification of the magnetic field in it changed. At all heights from 0 to 30000 km, the distribution of large-scale magnetic fields changed significantly.

4. MAGNETIC FIELDS AND MOTIONS IN FILAMENTS

If the large-scale distribution of background magnetic field structures and filament locations relative to them are considered, then the following peculiarities can be seen.

For the filaments separating the background magnetic fields of opposite signs, the magnetic field strength Br at the photospheric level under the filament is for the most part nonzero and a small-scale field of the same sign predominates. The strength Br under the filaments of this type is of the order of (5–10) G. Stable extended filaments for which the magnetic fields at the filament ends differ in sign, while the field strength in the central zone is zero or nearly zero are commonly observed (Martin, 1998). This can be seen from Fig. 2.

The branching of a filament, when it becomes V-shaped, is a common occurrence in its evolution. In this case, the relationship of the filament to the magnetic fields and the shape of the bright stripes near them change.

The distribution of photospheric motions of matter in filaments is mottled in pattern.

When the filaments in HeI are examined in detail, it turns out that most of the filaments are chains of separate dark knots. At first glance, comparison of the filament structure with the distribution of the radial photospheric magnetic field suggests that each knot is a small loop structure (or a small rope) whose "feet" rest on opposite-polarity magnetic field regions (bipolar structure). However, this interpretation of the nature of the dark knots may be simplified or even inaccurate. Comparison of the filaments observed in HeI and Hα suggests that, at least in some cases, the dark knots are the places in the filament from where peculiar branches (barbs) go off (for these filament structures, see, e.g., Martin, 1998). These branches go away from the filament into the chromosphere and, as some researchers believe (Martin and Echols, 1994), their ends lie in the magnetic field regions with nondominant (parasitic) field polarity for the corresponding region. The observations of filaments are commonly interpreted in such a way that the filament is a set of loop segments. According to the model by Marten and Zwaan (2001), such a filament emerges with the involvement of magnetic reconnection of some original magnetic ropes in the corona.

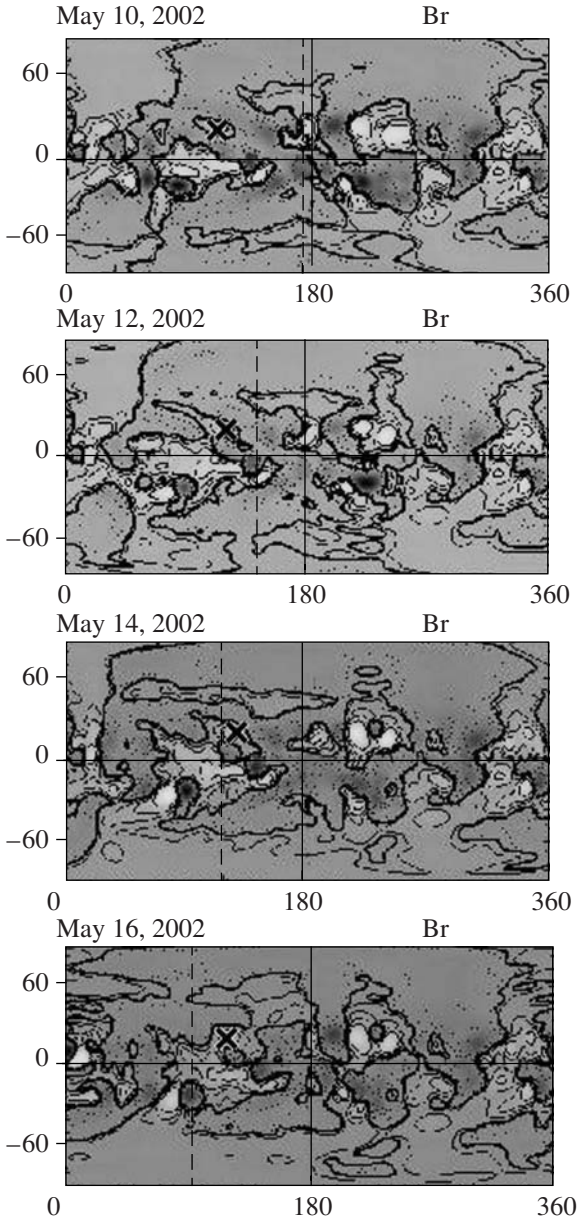

Fig. 12. Set of synoptic maps illustrating the change in the distribution of the large-scale magnetic field in the CH with time: May 10, 12, 14, and 16, 2002. The crosses indicate the geometrical CH centers.

Let us consider in more detail the magnetic field variation with height in an extended filament lying initially near the boundary of the opposite-polarity background field structures (filament no. 12 from the table). From May 15 to May 16, the filament stretched to the north and became more compact. Subsequently, it broke down into separate knots and only the middle part of the filament remained on May 20. A floccule was adjacent to the filament from the east; a bright

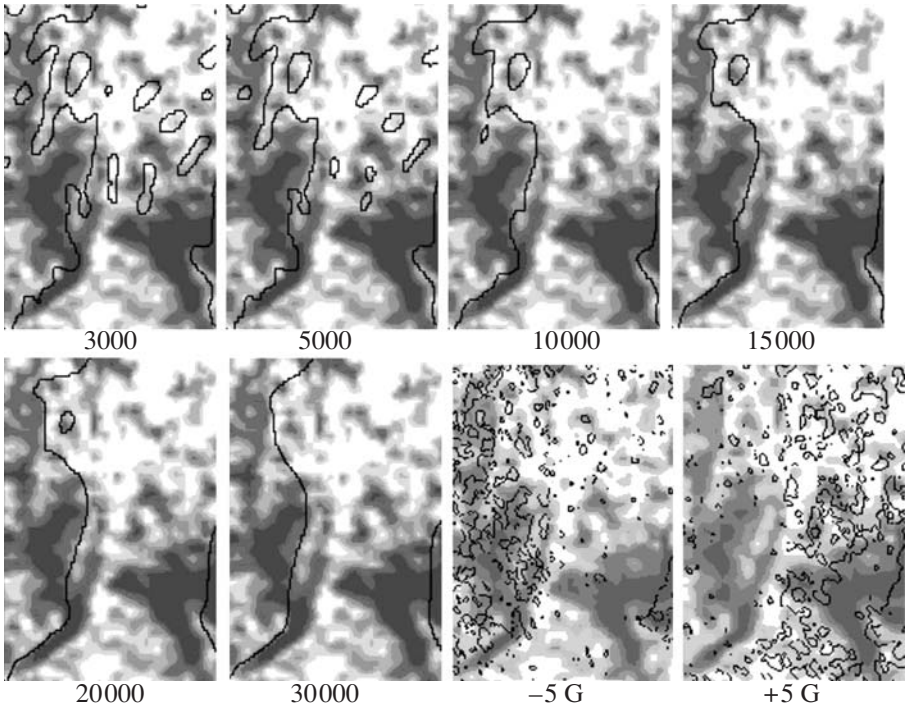

Fig. 13. Location of the zero line at various heights in the filament on May 15, 2002.

stripe was observed to the west from the filament, which transformed into a small CH in the north.

Just as was done for the CH, the calculated zero magnetic field lines at various heights from 3 to 30 thousand kilometers were superimposed on the filament images. The filament observations for five days, from May 15 to May 18 and on May 20, were analyzed. Figures 13 and 14 present the data for May 15 and 20, respectively.

Two processes are characteristic of the magnetic field development in the filament from May 15 to May 20: the displacement of the zero line separating the large-scale background field structures near the filament and the appearance and disappearance of dark knots constituting the filament. These processes proceeded differently in the northern and southern parts of the filament.

On May 15, the filament and the floccule lay in the S field at zero height (the height at which the magnetic field was measured). However, already at 3000 km, the zero line passed between them and the N field was above the filament. This location of the zero line was retained up to 30000 km.

The situation gradually changed with time. The zero line was displaced to the west and on May 17 the southern part of the filament was already in the S field from 10000 km. By May 20, the southern part of the filament disappeared, while its northern part lagged behind the floccule. Apart from the possible bending of the zero surface with height, its actual displacement over two or three days is also observed.

This change in the relative positions of the zero line and the filament can be explained in the following way. Here, two effects are probably superimposed. On the one hand, the zero surface that passes through the zero photospheric line and at all points of which the component calculated in the potential approximation $Br = 0$ is not radial. It is on this surface that the zero magnetic field lines calculated here at various heights and shown in Figs. 13 and 14 are located. The zero surface not just deviates from the radial direction, but is bent near the solar surface, including in longitude (Eselevich et al., 1999). As a result, the projection of the zero line from various heights onto the solar image in the HeI 10830 Å line may prove to be, for example, eastward of the filament, as in Fig. 13.

This effect could also be in action on May 20, 2002. In this case, however, the observed result can be determined by another phenomenon. The plane (or a more complex surface) in which the filament lies is not radial for most filaments. As a result, during the solar rotation, the apparent filament thickness becomes minimal not on the central meridian, but, as a rule, to the east of it (d'Azambuja et al. 1948). It thus follows that the filament located approximately along the meridian is inclined to the west. Zagnetko et al. (2005) showed that the surface near which the filament matter is mainly concentrated is close to the zero

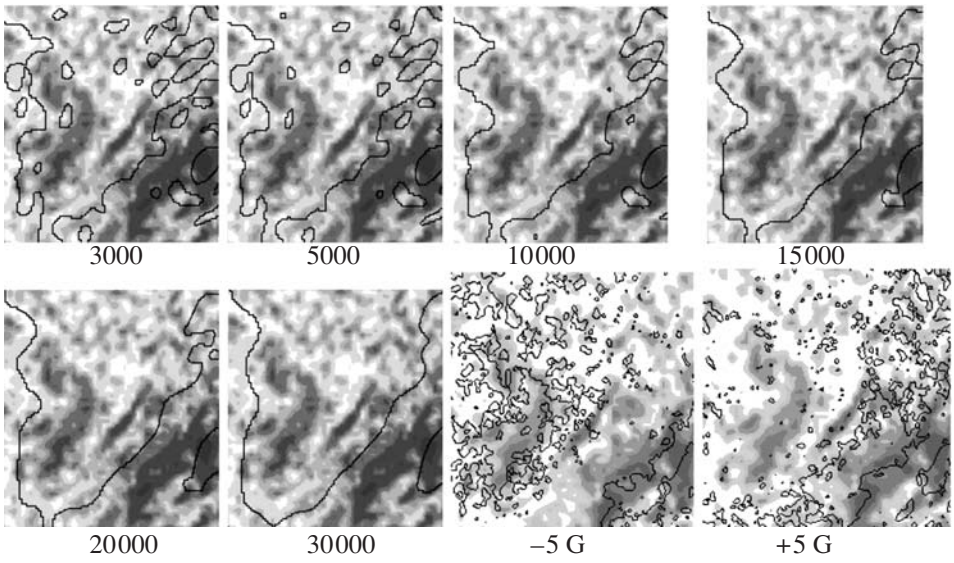

Fig. 14. Same as Fig. 13 for May 20, 2002.

surface. This is yet another argument that the zero surface is not radial. In this case, however, this surface deviates from the radial direction to the west. On May 15, 2002, the filament lay to the east of the central meridian and, judging by Fig. 13, near the longitude at which the filament reaches its minimum thickness. In this case, as the height increases, the projection of the zero line onto the solar disk should be near the projection of the filament, shifting only slightly from it to the west. However, since the first effect dominates, the projections of the zero lines from various heights onto the solar image were responsible for the displacement of these projections to the east of the filaments.

On May 20, 2002, the filament lay to the west of the central meridian. In this case, the second effect is probably crucial. We see that the projections of the zero lines onto the solar image in the HeI line were westward of the filament.

The heights to which the bipolar structures extend can be judged by the tortuosity of the zero line passing over the filament and the opposite-polarity field inclusions in the region under consideration (see Figs. 13 and 14). The results of such an analysis are presented in Fig. 15 separately for the two parts of the filament and the CH in which the northern part of the filament was located.

As we see, the magnetic field penetration heights change significantly from day to day and are different for different points of the same filament.

As regards the filament location at the boundary between the large-scale background field structures, the picture here is changeable.

5. CONCLUSIONS

Comparison of several types of data that we considered showed that our approach allows the processes that take place near filaments at various levels in the solar atmosphere, from the photosphere to the corona, to be studied comprehensively.

This is confirmed by the agreement between many of our conclusions and the previous results of other authors. This increases the reliability of the new results obtained here: the morphology of filament formation in a CH and emergence from it, the detailed picture of large-scale field variation at different heights above a CH, and the change in the vertical stratification of the magnetic field in an extended filament.

Based on the data used, we obtained the following results:

—Most of the filaments observed in the HeI 1083 nm line consist of dark knots with different velocity distributions in them. A possible interpretation of these knots is offered.

—The height of the small-scale magnetic field distribution near the individual dark knots of filaments in the solar atmosphere varies between 3000 and 20000 km.

—The zero surface separating the large-scale magnetic field structures in the corona and calculated in the potential approximation changes the inclination to the solar surface with height and is displaced in one or two days.

—The observed formation of a filament in a CH was accompanied by a significant magnetic field variation in the CH region at heights from 0 to 30000 km

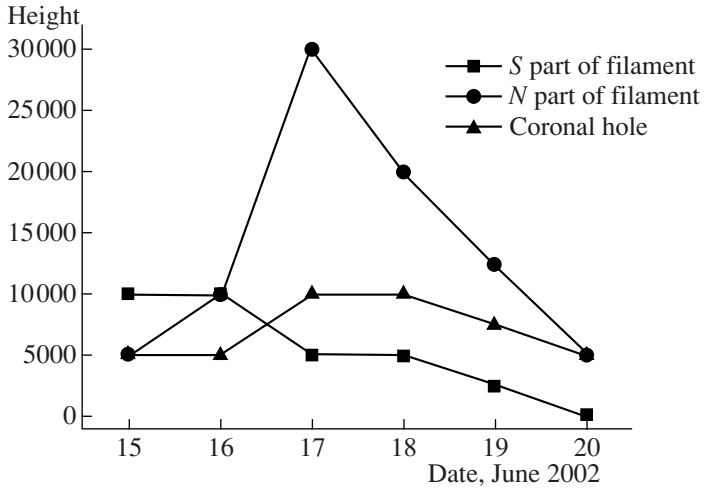

Fig. 15. Heights (km) to which the magnetic fields of the bipolar structures in the two parts of the filament and in the CH extended from May 15 to May 20, 2002.

up to the change of the predominant field sign over the entire CH area. We assume that this occurs at the stage of CH disappearance.

REFERENCES

1. V. Gaizauskas, *IAU Colloquium 167, ASP Conf. Ser.*, Ed. by D. Webb, D. Rust, and B. Schnieder, (1998), Vol. 150, p. 257.
2. d'Azambuja et al., Ann. Obs. Paris. Meudon **6**, Fasc. VII (1948).
3. V. G. Eselevich, V. G. Fainshtein, and G. V. Rudenko, Solar Phys. **188**, 277 (1999).
4. R. K. Zhigalkin, Izv. Krymsk. Astrofiz. Obs. **104** (2007) (in press).
5. I. A. Zhitnik, R. K. Zhigalkin, A. P. Ignat'ev, et al., Izv. Krymsk. Astrofiz. Obs. **101**, 128 (2005)
6. A. M. Zagnetko, B. P. Filippov, and O. G. Den, Astron. Zh. **82**, 474 (2005).
7. E. V. Malanushenko and N. N. Stepanian, Proc. Solar and Heliospheric Plasma Physics, Thessaloniki, Greece, (1996), p. 18.
8. Ps. Marten and C. Zwaan, Astrophys. J. **558**, 872 (2001).
9. S. Martin, Solar Phys. **182**, 107 (1998).
10. S. F. Martin and C. R. Echols, *Solar Surface Magnetism*, Ed. by R. J. Rutten and C. J. Schrijver (Kluwer Academic Publ., Dordrecht, Holland, 1994), p. 339.
11. G. Aulanier and B. Schmieder, Astron. Astrophys. **386**, 1106 (2002).
12. G. V. Rudenko, Solar Phys. **198**, 5 (2001).
13. N. N. Stepanian, E. V. Dolgopolova, A. I. Elizarov, et al., Izv. Krymsk. Astrofiz. Obs. **96**, 194 (2000).
14. B. P. Filippov, *Eruptive Processes on the Sun* (Fizmatlit, Moscow, 2007) [in Russian].
15. K. L. Harvey and V. Gaizauskas, *IAU Colloquium 167, ASP Conf. Ser.*, Ed. by D. Webb, D. Rust, and B. Schnieder (1998), Vol. 150, p. 269.